Spatio-temporal patterns of genetic variation in *Arbacia lixula*, a thermophilous sea urchin in expansion in the Mediterranean

Rocío Pérez-Portela [1, 2 *], Owen S Wangensteen [3], Alex Garcia-Cisneros [1], Claudio Valero-Jiménez [4], Cruz Palacín [5], Xavier Turon [1]

[1] Center for Advanced Studies of Blanes (CEAB, CSIC), Accès a la Cala Sant Francesc, 14, Blanes, Girona, Spain

[2] Current address: Department of Biology, Geology, Physics and Inorganic Chemistry, Rey Juan Carlos University, C/ Tulipán s/n, Móstoles, 28932, Spain

[3] Norwegian College of Fishery Science, UiT The Arctic University of Norway, Tromsø, Norway.

[4] Laboratory of Phytopathology, Wageningen University, 6708 PB, Wageningen, the Netherlands

[5] Department of Evolutionary Biology, Ecology and Environmental

Sciences, University of Barcelona, and Research Institute of Biodiversity (IRBIO), Avda. Diagonal, 643, Barcelona, Spain

* Corresponding author:

Rocío Pérez-Portela

Department of Biology, Geology, Physics and Inorganic Chemistry, Rey Juan Carlos University, C/ Tulipán s/n, Móstoles, 28932, Spain

Phone: +34 914887192

Fax: +34 916647490

Email: perezportela@gmail.com

Running title: Spatio-temporal genetics of a sea urchin in expansion

Word count: 6909

ABSTRACT

The genetic structure of 13 populations of the amphiatlantic sea urchin *Arbacia lixula*, as well as temporal genetic changes in three of these localities, were assessed using 10 hypervariable microsatellite loci. This thermophilous sea urchin is an important engineer species triggering the formation of barren grounds through its grazing activity. Its abundance seems to be increasing in most parts of the Mediterranean, probably favoured by warming conditions. Significant genetic differentiation was found both spatially and temporally. The main break corresponded to the separation of western Atlantic populations from those in eastern Atlantic and the Mediterranean Sea. A less marked, but significant differentiation was also found between Macaronesia (eastern Atlantic) and the Mediterranean. In the latter area, a signal of differentiation between the transitional area (Alboran Sea) and the rest of the Mediterranean was detected. However, no genetic structure is found within the Mediterranean (excluding Alboran) across the Siculo-Tunisian Strait, resulting from either enough gene flow to homogenize distance areas or/and a recent evolutionary history marked by demographic expansion in this basin. Genetic temporal variation at the Alboran Sea is as important as spatial variation, suggesting that inter-annual changes in hydrological features can affect the genetic composition of the populations. A picture of genetic homogeneity in the Mediterranean emerges, implying that the potential expansion of this

keystone species will not be limited by intraspecific genetic features and/or potential impact of postulated barriers to gene flow in the region.

Keywords: Population genetics, temporal trends, colonisation, divergence, gene flow, barrens

INTRODUCTION

Arbacia lixula (Linnaeus, 1758) is a warm-temperate water species occurring from the western Atlantic in Brazil (Tommasi, 1964) to the other side of the Atlantic where it is present in the Macaronesian archipelagos (Mortensen, 1935; Lessios *et al.*, 2012), African Atlantic coast from Gibraltar to Angola, and the Mediterranean Sea (Tortonese, 1965). Marine species with amphiatlantic distributions (i.e., those inhabiting both eastern and western Atlantic shorelines) provide interesting tests of the permeability of the mid-Atlantic dispersal barrier. Barring cases of cryptic speciation (e.g. Carmona *et al.*, 2011), historical, hydrological, and developmental features are usually called for to explain trans-Atlantic dispersal. In this sense, *Arbacia* is an interesting genus with fossil record dating from the Paleocene (Kroh and Smith, 2010). Its five extant species occur in the eastern Pacific and both sides of the Atlantic (Lessios *et al.*, 2012). The two Atlantic species, *A. punctulata* (western Atlantic) and *A. lixula*

(amphiatlantic) diverged some 1.5-3.3 mya at both sides of the mid-Atlantic barrier (Lessios *et al.*, 2012), likely by a range expansion event from western to eastern Atlantic of the lineage that would become *A. lixula*, which nevertheless crossed again the mid-Atlantic barrier to establish the present-day Brazilian populations (Lessios *et al.*, 2012; Wangensteen *et al.*, 2012).

Arbacia lixula is an ecosystem engineer species (i.e., those that change availability of resources to other species, Jones *et al.*, 1994, 1997), capable of transforming littoral communities into barren grounds due to its grazing activity (Bulleri *et al.*, 1999; Gianguzza *et al.*, 2011; Bonaviri *et al.*, 2011). Mitochondrial genetic data (Wangensteen *et al.*, 2012) and the absence of fossil records (Stefanini, 1911; Mortensen 1935; Madeira *et al.*, 2012) support the idea of a relatively recent colonisation of this sea urchin in the Mediterranean Sea, likely during the last interglacial period (Wangensteen *et al.*, 2012). The Mediterranean is a semi-enclosed sea subject to important anthropogenic impacts (e.g. Lejeusne *et al.*, 2009; Coll *et al.*, 2012). In turn, these threats interact in complex ways with the ongoing climate change that favours the progressive tropicalization of this sea (Francour *et al.*, 1994). Among the key drivers of structure and function in littoral Mediterranean communities is the grazing activity of sea urchins, which induce regime shifts between macroalgal beds and sea urchin barrens (Bonaviri *et al.*

2011). Human-derived impacts can exacerbate the risk and irreversibility of such dramatic changes (Ling *et al.*, 2015).

The thermophilous nature of *A. lixula* has long been recognized (Kempf, 1962; Tortonese, 1965), and this species is listed among those being currently favoured by the warming of the Mediterranean (Wangensteen, 2013a). Its abundance has been increasing in several areas of this sea in the past (Petit *et al.*, 1950; Boudouresque *et al.*, 1989; Francour *et al.*, 1994). Its reproduction is enhanced by high temperatures (Gianguzza *et al.*, 2011, Wangensteen *et al.*, 2013b) and larval development features indicate that warming, modulated by other factors such as pH and food availability, may favour *A. lixula* development (Privitera *et al.*, 2011; Wangensteen *et al.*, 2013a; Gianguzza *et al.*, 2014; Visconti *et al.*, 2017). Although recent results showed a regression of marine invertebrate populations at the coast of Israel (eastern Mediterranean) due to the whole ecosystem collapsing (Yeruham *et al.*, 2015; Rilov, 2016), the general scenario is a progressive increase of abundance of *A. lixula* in most areas of the Mediterranean (Privitera *et al.*, 2011; Wangensteen, 2013a; Visconti *et al.*, 2017), which will result in significant changes in ecosystem functioning.

Under this scenario, it is of utmost importance to ascertain the genetic structure of *A. lixula*. In a previous study, Wangensteen *et al.* (2012) identified phylogeographic patterns in *A. lixula* using sequences of the

123 mitochondrial gene cytochrome oxidase I (COI). That study identified three
124 haplogroups in worldwide populations, one of them shared between eastern
125 and western Atlantic populations. The mitochondrial structure of the species
126 appeared to be shaped by Pleistocene demographic expansions, isolation
127 between the eastern Atlantic, western Atlantic and Mediterranean Sea, and
128 genetic homogeneity across the Mediterranean. Nevertheless, the lack of
129 genetic differentiation across the Mediterranean basin (Wangensteen *et al.*
130 2012; Deli *et al.*, 2017) needs to be compared with nuclear markers to
131 confirm the information on gene flow patterns and genetic signals in this
132 species. Mitochondrial DNA only retains half of the species' evolutionary
133 history (Avise, 2000), and due to the potential differential selection (Silva *et*
134 *al.*, 2014; Consuegra *et al.*, 2015) and stochasticity of the coalescence
135 processes between nuclear and mitochondrial DNA, these two types of
136 markers can show different evolutionary signatures (e.g. Glynn *et al.*, 2015;
137 Garcia-Cisneros *et al.*, 2016; Pérez-Portela *et al.*, 2017). Therefore,
138 combining both mitochondrial and nuclear information should provide
139 complementary information to unravel both recent and historical processes
140 shaping the genetic structure of *A. lixula*.
141 Population analyses should additionally include information about temporal
142 changes in genetic make-up to understand whether the structure observed is
143 stable over contemporary time periods. Currently, there is still a scarce
144 number of temporal genetic studies in marine species, despite being a

fundamental information for interpreting their long-term genetic distribution (e.g. Pérez-Portela *et al*., 2012; Pineda *et al*., 2016; Pascual *et al*., 2016). It is known that the stochasticity of reproduction, recruitment and survival of larvae and juveniles can potentially change the genetic composition of populations over the generations (e.g. Calderón *et al*., 2012; Aglieri *et al.*, 2014; Couvray and Coupé 2018). Additionally, temporal variation across oceanographic discontinuities can also promote variation of gene flow patterns over time (Olivar *et al*., 2003; Calderón *et al*., 2012). An outstanding example of inter-annual oceanographic variation is that across the Atlantic-Mediterranean transition, associated with shifts in Atlantic and Mediterranean water contributions across the Alboran Sea (Renault *et al.*, 2012; Oguz *et al.*, 2014). These marine circulation variations determine different levels of genetic mixing between Atlantic and Mediterranean genetic stocks over the years (Pascual *et al*., 2016). Therefore, spatio-temporal structuring patterns can provide valuable information about the future evolution of the populations, identifying connectivity patterns over time, and reservoirs of genetic diversity, among other important features.

In the present work, we use hypervariable nuclear microsatellite loci to investigate in detail the genetic structure of *A. lixula* across most of its distribution range using the same samples analysed by Wangensteen *et al.* (2012), but also extending these analyses to a temporal perspective. With new nuclear markers and samples, we specifically tested: a) the disruptive

effect of major oceanographic breaks, including the mid-Atlantic barrier, as well as migration patterns across them, which were used to determine the coherence of genetic divergence patterns between the nuclear and mitochondrial data, and b) the relevance of the genetic change over time in two sites at the Alboran Sea (Atlantic-Mediterranean transition) and in another non-transitional Mediterranean site, which were sampled at two time points. We were particularly interested in inferring spatio-temporal population structure at the Atlanto-Mediterranean transition where other marine invertebrates have shown significant inter-annual variation in genetic structure (Pascual *et al.*, 2016). The data generated in this study can be useful to infer present-day and future processes in the ongoing expansion of this keystone engineer species.

MATERIAL AND METHODS

Sample collection and microsatellite genotyping

Specimens of *A. lixula* were collected by SCUBA diving from 13 different localities across most of the distribution range of the species.

186 "*Spatial genetic structure"*: The collection sites included two localities on
187 the western Atlantic (Brazil), three sites on the eastern Atlantic: Cape
188 Verde, Canary Islands and Azores (Macaronesian Islands), five at the
189 western Mediterranean (including two populations from the transitional
190 zone at the Alboran Sea), and three in the eastern Mediterranean (see details
191 in Figure 1 and Table 1). These samples correspond to a subset of 278 out of
192 604 individuals previously sequenced (mitochondrial COI gene) by
193 Wangensteen *et al.* (2012) between 2009 and 2011, with an additional
194 location from Sicily collected for the present study at the end of 2011. This
195 sampling scheme included several major oceanographic breaks and/or
196 transitions with observed disruptive effect in populations of other
197 echinoderms (e.g. Calderón *et al*., 2008; Taboada and Pérez-Portela 2016;
198 Garcia-Cisneros *et al*., 2016, 2017; Pérez-Portela *et al*., 2017): the mid-
199 Atlantic barrier that divides the eastern and western Atlantic; the Gibraltar
200 Strait that marks the geographical partition between the Atlantic Ocean and
201 Mediterranean Sea; the Almeria-Oran front, described as the
202 biogeographical break between the Atlantic and Mediterranean basins in
203 most marine species; and the Siculo-Tunisian Strait between the eastern and
204 western Mediterranean sub-basins.

205 "*Temporal genetic trends*": For testing potential changes in genetic structure
206 and diversity over time, three of the Mediterranean populations sampled in
207 2009 were re-sampled in 2014: Colera at the northwestern Mediterranean,

208 and La Herradura and Torremuelle at the Alboran Sea- Atlantic-
209 Mediterranean transition. These sites were selected because we were
210 specifically interested in exploring the potential effect of inter-annual
211 oceanographic variation on populations' divergence at the Atlantic-
212 Mediterranean transition, an area where *A. lixula* populations displayed
213 significant mitochondrial differences (Wangensteen *et al*. 2012) despite the
214 short geographical distances separating them to other Atlantic and
215 Mediterranean sites. We analysed the two Alboran sites for which samples
216 from 2009 were available (Wangensteen *et al.* 2012) and one northwestern
217 Mediterranean site far away from this Atlantic-Mediterranean transition for
218 comparison with the first two sites.

219 Tissue samples were collected and fixed as described in Wangensteen *et al*.
220 2012. Total DNA was extracted from 302 individuals for the "spatial" study,
221 plus 77 individuals of the 2014 sampling used for the "temporal" study. The
222 REDExtract-N-Amp Tissue PCR kit (from Sigma-Aldrich,
223 www.sigmaaldrich.com/) was used, following the protocol described by the
224 manufacturer. All individuals were genotyped at 10 microsatellite loci
225 (ALM2, ALM4, ALM5, ALM7, ALM8, ALM9, ALM11, ALM14, ALM15
226 and ALM17) described in Garcia-Cisneros *et al.* (2013).

227 Amplification of fragments containing microsatellites was performed by
228 Polymerase Chain Reaction (PCR) in a final volume of 10 μL, containing 5

229 µl of ReadyMix Taq PCR Reaction Mix (Sigma-Aldrich), 2-8 µg of DNA,
230 0.4 µl (10µM) of each primer (forward and reverse) and 3.2 µl of ultrapure
231 water. Samples were amplified in a thermocycler (Bio-Rad MyCycler,
232 http://www.bio-rad.com) with an initial 2 minutes denaturation step at 94°C,
233 and 35 amplification cycles: 45 seconds at 94°C, 50 seconds at the locus
234 specific annealing temperature (51-58°C; see Garcia-Cisneros *et al.,* 2013)
235 and 40 seconds at 72°C, followed by 4 minutes of final extension at 72°C.

236 Successful amplifications were genotyped in an automated sequencer
237 (Applied Biosystems, www.thermofisher.com) in the Science and
238 Technology Centres of the University of Barcelona (CCiTUB). Allele
239 length was estimated relative to the internal size standard 70-500 ROX
240 (Bioventures) using the software Peak-Scanner v 1.0 (Applied Biosystems).

241

242 **Data analyses**

243

244 The number of alleles per population, observed heterozygosity (Ho),
245 expected heterozygosity (He), inbreeding coefficients (F_{IS}), and number of
246 private alleles per geographical area were calculated using GenAlex v 6.41
247 (Peakall and Smouse, 2006) and Genepop v 4.2 webserver (Raymond and
248 Rousset 1995). The exact test for departure from Hardy-Weinberg

249 Equilibrium (HWE) was performed in Arlequin v 3.5.1.2 (Excoffier *et al.*,
250 2005). The potential correlation between the F_{IS} and number of missing data
251 per population was explored to understand the impact of missing data on
252 this statistic.

253

254 *Spatial genetic structure*

255 We used different approaches based on Bayesian clustering, genetic
256 distances, and discriminant analyses of principal components. Whereas
257 methods based on genetic distances (e.g F_{ST}) are affected by the
258 populations' Hardy-Weinberg disequilibrium, and assume absence of
259 linkage disequilibrium among all loci within populations, other multivariate
260 methods are free from these two assumptions. Therefore, we compared here
261 different methods to minimise potential bias of using only one approach.

262 The software STRUCTURE v 2.3.4 (Pritchard *et al.*, 2000) was used to
263 infer an optimal number of homogeneous genetic units (K) based on
264 Bayesian clustering analyses. It was run with the whole dataset, with a K
265 number from 1 to 16, and 200,000 Markov chain Monte Carlo (MCMC)
266 steps were performed following 80,000 burn-in iterations in 10 independent
267 replicates under the "admixture model" and the "correlated allele
268 frequencies mode" implemented by the software. The same strategy was

separately applied to selected subsets of the populations in order to obtain a finer-scale analysis within major marine areas: a) the eastern Atlantic and Mediterranean populations to better explore genetic partition across the Atlantic-Mediterranean arch and, b) only Mediterranean sites to investigate potential divergence within this basin and across the Almeria-Oran Front and the Siculo-Tunisian Strait. The most likely value of 'real' clusters was identified comparing the rate of change in the likelihood of K. The optimal K values were determined using the *ad hoc* statistic ΔK (Evanno *et al.*, 2005). Ten independent replicates per run were averaged using the clumpak server (Kopelman *et al.*, 2015), and results were graphically represented with the same software.

Genetic clusters were also delineated using "find.clusters" of the adegenet package for R software (Jombart, 2008; Team R Core, 2013) using a K-means clustering algorithm. A range of cluster numbers was chosen and the optimal number was selected using a Bayesian Information Criterion (BIC). Group assignment probabilities were then displayed with the "compoplot" function of adegenet. As before, further analyses were performed with "find.clusters" considering only eastern Atlantic and Mediterranean populations and, finally, only Mediterranean populations. Additionally, we ran a discriminant analysis of principal components (DAPC, Jombart *et al.*, 2010) using populations as groups with the adegenet package. This method allows the visual identification of genetic clusters of individuals and can

outperform Bayesian clustering approaches in detecting genetic substructure (Jombart *et al.*, 2010). The optimal number of principal components (PC) from the PCA step passed onto the discriminant analysis was determined by the cross-validation method, and by comparison of a-scores for a set of increasing numbers of PCs and a spline interpolation using the "a-score" function of adegenet. DAPCs were performed separately for the whole dataset, for the eastern Atlantic plus Mediterranean populations, and for the Mediterranean populations alone.

The software Arlequin was used to estimate population distances with the F_{ST} statistic between pairs of populations based on an allele infinite model. The Jost's D_{est} estimator (Jost, 2008) was also obtained with the package DEMEtics in R (Gerlach *et al.*, 2010). A false discovery rate (FDR) correction was applied for the p-values (Benjamini-Yekutieli method, Narum, 2006) to account for multiple tests. The genetic dissimilarity matrices generated with both estimators were represented with cluster analyses and heatmaps obtained with the gplots package for R (Warnes *et al.*, 2016).

To test the concordance between nuclear and mitochondrial genetic distances, we performed correlation analyses for F_{ST} and D_{est} matrixes obtained from microsatellite loci (this study) and COI sequences (COI distance matrixes obtained from Wangensteen *et al.*, 2012).

312 Null allele frequencies were estimated following the Expectation
313 Maximization (EM) algorithm implemented in FreeNA (Chapuis and
314 Estoup, 2007). Using this information, the corrected estimations of F_{ST}
315 values were calculated applying the *ENA* and *INA* methods with the same
316 software.

317 Analyses of molecular variance (AMOVA) were computed using an allele
318 infinite model, and their significance tested with 20,000 permutations in
319 Arlequin. For the AMOVAs we grouped populations in different sets
320 according to the F_{ST} results, geographical origin and known oceanographic
321 barriers. We initially tested differences among western Atlantic, eastern
322 Atlantic and Mediterranean Sea, considering two major marine breaks: the
323 mid-Atlantic barrier and the Gibraltar Strait. In a second analysis we
324 removed populations from western Atlantic and compared east Atlantic
325 populations with Mediterranean populations. We then compared the
326 populations from the Alboran Sea with the rest of the Mediterranean to test
327 differentiation across the Almeria-Oran front. Finally, we analysed only
328 Mediterranean populations excluding Alboran Sea, comparing the eastern
329 and the western sub-basins to explore the potential disruptive effect of the
330 Siculo-Tunisian Strait.

331 The potential effect of genetic isolation of populations by geographical
332 distance, independently of oceanographic barriers, was assessed for the

whole dataset, and separately for different population subsets (eastern Atlantic and Mediterranean Sea, and only the Mediterranean Sea), using the correlation of linearized genetic distances (F_{ST} /1– F_{ST}) with geographical distances (as measured in Wangensteen *et al.*, 2012) between localities. The significance of the correlations was tested by a Mantel test, as implemented in Arlequin with 20,000 permutations per analysis.

To estimate gene flow among marine areas, we calculated mutation-scaled effective migration rates (M) based on Bayesian inference using the software MIGRATE v 3.6.11 (Beerli 2006; Beerli and Felsenstein 2001). We estimated asymmetric M among the three major geographical areas: the western Atlantic (Brazilian sites), eastern Atlantic (Macaronesian islands) and the Mediterranean Sea. Migration estimates per generation can be expressed as 4N*m* for nuclear markers, in which N is the effective population size and *m* the immigration rate. Three preliminary runs were performed to infer initial parameters and check convergence before performing a final run. For the latter, we used a Brownian motion mutation model with constant mutation rate for all loci, three different replicates with one long chain, 3,000,000 iterations (9,000,000 final sampled parameters) with the first 30,000 iterations discarded, and an adaptive heating scheme of four different temperature chains.

Temporal genetic trends

For the three populations sampled in 2009 and again in 2014 (Colera, Torremuelle and La Herradura), we computed a DAPC representation using populations from each sampling year as groups (with the adegenet package in R) and pairwise tests using F_{ST} (calculated with Arlequin) and D_{est} (calculated with DEMEtics) as described above.

We also estimated effective population sizes (Ne) for these three populations (Colera, Torremuelle and La Herradura) using the temporal method, based in shifts in allele frequencies between samples taken a number of generations apart (Jorde and Ryman 2007). We used NeEstimator v.2.01 (Do *et al.* 2014) to calculate Ne based on allele frequency changes between the two sampling years using three different estimators that differ in precision and bias (Do *et al.* 2014): those of Nei and Tajima (1981), Pollak (1983), and Jorde and Ryman (2007). We considered a generation per year (Wangensteen *et al.* 2013b) and removed alleles below a frequency threshold of 0.05 to reduce random error (likely at the cost of a slight downward bias in the estimates, Do *et al.* 2014). *Arbacia lixula* has overlapping generations, which adds complexity to the computation of Ne estimates originally devised for discrete generations. Ideally, a correction should be made on measures of temporal change in allele frequency that incorporates the different contributions of the co-existing cohorts (Jorde and Ryman 1995). Calculating this correction requires precise biological knowledge of the cohort structure, age-specific survival rates, and age-

specific reproduction rates (e.g., Calderón *et al.* 2009), parameters that were not available for *A. lixula*. We nevertheless applied temporal methods without correction as, first, we sampled the sea urchins randomly with respect to age and, second, we sampled at a wide interval of generations (5 generations apart, from 2009 to 2014). Jorde and Ryman (1995) showed how sampling over long time intervals greatly reduces the bias in temporal methods for overlapping generations. In any case, our estimates should still be useful for comparative purposes among populations, as biological parameters are unlikely to be very different between populations and, therefore, any remaining bias should be similar.

RESULTS

The 10 microsatellite loci were highly polymorphic, with a total number of alleles ranging between 16 (locus ALM11) and 38 (locus ALM4). Details of genetic descriptors for each locus and population are presented as supplementary material (Table S1). Populations of *A. lixula* were in general characterised by high genetic diversity and a large number of alleles (mean number per locus ranged from 9.3 to 14.3 alleles, Table 1). Allele richness, used to compare allelic diversity among marine areas with large differences in sample size, showed that the eastern Atlantic retained the highest richness, followed by the Mediterranean and the western Atlantic areas.

Regarding private alleles, the eastern Atlantic showed the lowest value, with only 6.77% (13 alleles) of private alleles, whereas the Mediterranean and western Atlantic had 14.2% (31 alleles) and 10.7% (14 alleles) of private alleles, respectively (Supplementary Fig. S1).

In all populations observed heterozygosity was lower than expected, as demonstrated by the significant values of the F_{IS}, with significant deviation from the Hardy-Weinberg equilibrium in all populations ($p < 0.001$) (see Table 1). All microsatellite loci considered individually had overall positive values of F_{IS}, significant in all cases (F_{IS} values > 0.11) except in the locus ALM2 ($F_{IS} = 0.021$, $p = 0.157$). A low overall percentage of missing data (2.25%), distributed across all microsatellites but mostly concentrated in the Brazilian populations, makes unlikely that null alleles underlie this general deficit of heterozygotes. Interestingly, the two populations showing the highest percentage of missing data also displayed the lowest F_{IS} values, also suggesting that missing data are not related to positive and significant F_{IS} (Supplementary Fig. S2).

The Bayesian analyses detected an optimal K value of 3 based on the ΔK plot (Supplementary Fig. S3). The composition of the different populations in terms of these three genetic groups (sum of individual membership probabilities to each group) is represented in form of pie charts in Fig. 1A. One of the three genetic clusters detected sharply separated the populations

418 from the western Atlantic (yellow group in Fig. 1), while the rest of
419 populations were mainly composed of the other two genetic clusters. In
420 most individuals, however, the most probable group had a membership
421 probability above 75%, with few admixed individuals (Fig. 1B).

422 The situation is similar when genetic groups are delineated using the
423 "find.clusters" function in adegenet. The number of clusters (BIC criterion)
424 that better explains our data is 6 (Fig. S4), but the plot of membership
425 probabilities shows clear differences between western Atlantic and all other
426 Atlantic and Mediterranean samples, and some differentiation between the
427 eastern Atlantic (Macaronesia) and Mediterranean based on group
428 membership (Fig. S4). Hence, both the Bayesian clustering analysis and
429 "find.clusters" function detected a strong disruptive effect of the mid-
430 Atlantic barrier and a smaller effect of the eastern Atlantic (Macaronesia)-
431 Mediterranean transition. Analyses performed separately for the different
432 marine areas, the whole dataset, eastern Atlantic and Mediterranean and
433 only Mediterranean Sea, did not provide additional information (results not
434 shown).

435 Results from FreeNA showed that, in most cases, the correction of F_{ST}
436 values was minimal and the significance of the F_{ST} statistic did not change
437 in any case. Therefore, we consider that null alleles do not have a large
438 effect on genetic distance estimations in this study, and that uncorrected

values can be used for further analyses. The values of population differentiation using F_{ST} and D_{est} estimators are shown in Table S2 and graphically depicted as dendrograms and heatmaps in Fig. 2. Both estimators provide basically the same information, and are highly correlated ($r = 0.979$, $p < 0.001$). Moreover, they are highly correlated with previous genetic distance results from mitochondrial DNA obtained from Wangensteen *et al*. (2012) ($r = 0.832$ and $r = 0.816$, $p<0.01$ for F_{ST} and D_{est} values, respectively), showing congruent results between microsatellites and COI. Pairwise comparisons using microsatellite loci showed significant differentiation in all comparisons involving Brazilian populations (western Atlantic) with the rest, indicating a strong disruptive effect of the mid-Atlantic barrier. In addition, 17 comparisons (out of 24) between eastern Atlantic (Macaronesian) and Mediterranean populations were significant with both estimators, and 6 comparisons (out of 12) of the Alboran Sea populations (La Herradura and Torremuelle) with the rest of the Mediterranean were also significant for both indices, suggesting limited gene flow across two additional marine barriers: the Gibraltar Strait and the Almeria-Oran front. Furthermore, the two sites from the Alboran Sea, the transition area between the eastern Atlantic and Mediterranean Sea, were significantly different from each other for both indices. Only one significant pairwise difference within Macaronesia was found between Los Gigantes (Gig- Canary Islands) and Boavista (Cav- Cape Verde Islands) with Jost's

estimator (D_{est}). No significant divergence was found in any comparison within the western Atlantic. Within the Mediterranean Sea, no significant divergence was detected between sites, discarding the Siculo-Tunisian Strait as a genetic barrier in this species.

The heatmaps and dendrograms show clearly the distinction between western Atlantic populations and the remaining ones. Among the latter, the Macaronesian populations (eastern Atlantic- Faials, Los Gigantes and Boavista) formed a cluster, while Mediterranean populations appeared well mixed, with no inter-basin structure, although Alboran Sea populations (Torremuelle and La Herradura) were in general slightly more differentiated. In particular, the Torremuelle population was somewhat more divergent and was separated from the rest of Mediterranean populations (D_{est}) or even external to the eastern Atlantic plus Mediterranean clusters with the F_{ST} estimator (Fig. 2).

The spatial representation of the DAPC considering all populations (Fig. 3A, 51 PCs retained) showed again this pattern of separation between western Atlantic and eastern Atlantic plus Mediterranean in the first axis, while along the second axis the populations of the Macaronesian archipelagos are separated, albeit with some overlap, from the Mediterranean populations.

A DAPC graph excluding the Brazilian populations (Fig. 3B, 28 PCs retained) also showed a separation of the Macaronesian populations along the first axis, with overlap of the inertia ellipses. Torremuelle appeared also partially separated from the rest on the second axis. Finally, a DAPC considering only the Mediterranean populations (Fig. 3C, 26 PCs retained) showed less differentiation than the previous graphs. The two populations from the Alboran Sea appeared somewhat offset from the others, Torremuelle at one extreme of the first axis, La Herradura at one extreme along the second axis. No differentiation was apparent among populations of eastern and western Mediterranean, which showed interspersed centroids and widely overlapping inertia ellipses.

The results of the AMOVA analyses are coherent with the results from clustering and ordination methods (Table 2). An AMOVA considering as groups the Brazilian (western Atlantic), Macaronesian (eastern Atlantic), and Mediterranean populations (thus including the whole dataset) showed low but highly significant percentage of variation between groups and among populations within groups. The same outcome was found when excluding western Atlantic populations and considering the Macaronesian (eastern Atlantic) and the Mediterranean populations as different groups. However, in an analysis comparing the Alboran Sea with the rest of the Mediterranean populations the “among group” component explained only 0.54% of the variance and was not significant, while the among populations

504 within groups component was still significant (p = 0.002). Finally, if we
505 restrict the analysis to the Mediterranean populations excluding the Alboran
506 Sea and compare western with eastern Mediterranean populations, the
507 “among group” and the “among populations within groups” components
508 were not significant (p = 0.393 and p = 0.472, respectively), pointing to a
509 lack of gene-flow restriction across the Siculo-Tunisian Strait. In all cases,
510 most of the variation was contained within populations (29.32 - 32.58%)
511 and, particularly, within individuals (F_{IT}) (66.58 - 67.51%).

512 Assessing the hypothesis of isolation by distance through the Mantel test
513 revealed significant correlation between genetic and geographic distances (*r*
514 = 0.859, p < 0.001) when considering all populations. The correlation was
515 weaker, but still significant, when removing the Brazilian populations (*r* =
516 0.384, p = 0.025), and no correlation was found when considering just the
517 Mediterranean Sea (*r* = 0.189, p = 0.179) (see correlation graphs in
518 Supplementary Fig. S5).

519 The results of migration patterns between western Atlantic, eastern Atlantic
520 and Mediterranean Sea are presented in Table 4. Migration outputs showed
521 a general overlapping of the 95% confidential intervals around the M
522 estimates between areas. Only M estimations from the Mediterranean to
523 eastern Atlantic, and from the Mediterranean to the western Atlantic, which
524 were also the highest values of M (mean 24.182 and 18.336, respectively),

525 did not include zero within the confidence interval. These results may
526 suggest a potential pattern of asymmetric and long distance migration that
527 mainly occurs westwards. All the other estimations presented lower values
528 of the M mean, ranging from 7.145 to 14.919, and wide confidence intervals
529 that always included zero.

530

531 *Temporal genetic trends*

532 For the three populations that were re-sampled in 2014 (Torremuelle and La
533 Herradura at the Alboran Sea, and Colera at the northwestern
534 Mediterranean), the discerned genetic diversity was higher than that
535 recorded in 2009, in terms of observed heterozygosity and mean allele
536 number (except Colera for the latter parameter). Likewise, F_{IS} values were
537 lower, likely indicating less inbreeding (Table 1). Both F_{ST} and D_{est}
538 estimators showed significant genetic differentiation between Torremuelle
539 and the other two populations in 2009 ($p<0.015$), whereas La Herradura and
540 Colera did not show significant differences between them in 2009. In 2014,
541 the three populations displayed no significant differences in genetic
542 structure (Supplementary Table S3). Genetic distances also revealed that the
543 northwestern Mediterranean population of Colera did not significantly
544 change in genetic structure between 2009 and 2014, whereas both
545 populations at the Alboran Sea, Torremuelle and La Herradura,

546 demonstrated significant differences in genetic structure between 2009 and
547 2014. Therefore, Alboran Sea populations significantly changed their
548 genetic structure over time (Supplementary Table S3 for F_{ST} and $D_{est,}$ and
549 Figure 4). Mean differentiation values between years in the three
550 populations (F_{ST}: 0.040 ± 0.015, D_{est}: 0.103 ± 0.029, mean ± SE) were
551 higher, but of the same order, than mean genetic divergence detected in the
552 spatial study among the Mediterranean populations (F_{ST}: 0.015 ± 0.002, D_{est}:
553 0.087 ± 0.007, mean ± SE).

554 A heatmap representation of the F_{ST} and D_{est} values (Fig. 4A) highlighted
555 this pattern of marked interannual differences, but showed also that the three
556 populations were more divergent among them in 2009 than in 2014. A
557 DAPC representation (Fig. 4B, 20 PCs retained) revealed this same pattern:
558 the three populations were more separated in 2009 (particularly Tor), but
559 clustered tightly in 2014.

560 Considering one generation per year, the different estimators of effective
561 population size (Table 4) revealed low values in all populations
562 (approximate range 30 - 400 individuals). There were consistently higher
563 sizes in the northern population of Colera (177.3 - 387.9 individuals,
564 according to the different methods) than in the Alboran sea populations of
565 La Herradura (33.9 - 38.3) and Torremuelle (34.2 - 38.8). The three
566 estimators yielded remarkably similar estimates (and confidence intervals)

567 in the southern populations, but varied by a factor of ca. 2 for the Colera
568 population, for which defined confidence intervals could be obtained only
569 with the unbiased Jorde/Ryman's estimator.

570

571 **DISCUSSION**

572 The amphiatlantic sea urchin, *Arbacia lixula* displayed significant nuclear
573 divergence among the western Atlantic, eastern Atlantic and Mediterranean
574 Sea. Additionally, variable structure across the transitional area of the
575 Alboran Sea was also detected, which can be attributed to the inter-annual
576 variation in the oceanographic circulation across this area.

577 Populations of *A. lixula* showed a high degree of genetic diversity. There
578 was, however, a strong deficit of heterozygotes in all populations, with
579 significant departure from HWE. This is unexpected for species with long
580 pelagic larval duration. However, Addison and Hart (2005), reviewing data
581 for 124 marine invertebrates, showed a prevalence of positive F_{IS} values
582 even in species with planktonic larvae. It can be explained by several
583 factors, such as null alleles, mating among relatives, or unrecognized spatial
584 and temporal structure within samples (Wahlund effects). The scarcity of
585 null alleles indicates that our result is not an artefact of the markers. A
586 potential explanation in our case is that assortative mating occurs linked to

587 different gamete recognition proteins. Bindin, the sperm protein implicated
588 in the fertilization of the egg, is well known in sea urchins (Metz *et al*.,
589 1998; Zigler and Lessios, 2003; Zigler *et al.*, 2005; Lessios *et al.*, 2012).
590 Calderón and Turon (2010) showed that assortative mating linked to
591 selected positions in the bindin gene of *Paracentrotus* explained inter-cohort
592 differentiation. Such non-random mating structures, as well as the presence
593 of spatial breeding groups, linked to stochasticity in reproductive success,
594 patchiness in gamete distribution and the collective dispersal of genetically
595 related larvae in the plankton (e.g. Broquet *et al*., 2013; Couvray and Coupé
596 2018), can explain the lack of HWE detected *Arbacia*. In *A. lixula*, as in
597 many other species, most genetic diversity was retained within populations
598 and individuals (e.g. Calderón *et al*., 2008; Garcia-Cisneros *et al*., 2016).

599 Our nuclear results showed a sharp divergence between the western and
600 eastern Atlantic areas, likely due to the combined effect of isolation by
601 distance and the strong disruptive effect of the deep mid-Atlantic barrier.
602 This sharp genetic divergence is similar to the one observed in other
603 amphiatlantic echinoderms with large dispersal potential (e.g. Lessios *et al*.,
604 2001; Garcia-Cisneros *et al*., 2017). The nuclear divergence in *A. lixula* was
605 also largely congruent with COI mitochondrial data, but historical migration
606 patterns and allele frequencies highlighted interesting insights in its
607 phylogeography. Lessios *et al*. (2012) and Wangensteen *et al*. (2012)
608 hypothesised the colonization of the western Atlantic coast, across the mid-

609 Atlantic barrier, from eastern Atlantic stocks. However, neither migration
610 nor allele distribution patterns from our new nuclear results fully supported
611 this hypothesis and suggested instead the Mediterranean as a potential
612 source of colonizers. Migration patterns estimated from microsatellites
613 showed asymmetric gene flow among areas, with the most important
614 historical migration likely flowing westward from the Mediterranean to the
615 eastern and western Atlantic. Our results discard large historical
616 connectivity between eastern and western Atlantic regions, which showed a
617 low value of M. In addition, the Mediterranean origin of the western
618 Atlantic populations can be also supported by 14 alleles shared (out of 250)
619 between these two areas, whereas only two alleles were found in common
620 between the eastern and western Atlantic stocks that can be indicative of
621 long-term isolation between populations at both sides of the Atlantic.
622 Interestingly, a detailed re-evaluation of the COI network also points out the
623 potential origin of the Brazilian haplotype cluster from some of the most
624 frequent Mediterranean haplotypes. Therefore all current genetic evidences
625 suggest divergence of the western Atlantic populations of *A. lixula* from the
626 Mediterranean area, which likely happened after the Pleistocene
627 colonization and demographic expansion in the Mediterranean Sea (93.8–
628 205.2 kya) (Wangensteen *et al*., 2012). Nonetheless, further investigations
629 are necessary to discard other unexplored genetic stocks and to confirm the
630 Mediterranean origin of the western Atlantic lineages.

631 Additionally, subtler structure is also found in the Atlantic-Mediterranean
632 area, with significant differentiation between the Macaronesian islands and
633 the Mediterranean. The biogeographic break between Atlantic and
634 Mediterranean leaves a strong signature in the genetic structure of many
635 species of fish and invertebrates with different biological characteristics
636 (Patarnello *et al*., 2007; Pascual *et al.*, 2017), including sea urchins, sea
637 stars, brittle-stars and sea cucumbers (Borrero-Pérez *et al*., 2011; Pérez-
638 Portela *et al*., 2010; Calderón *et al*., 2012; Taboada and Pérez-Portela 2016;
639 Garcia-Cisneros *et al*., 2016, 2017). However, the Mediterranean Sea also
640 has a number of internal oceanographic barriers that can restrict species
641 dispersal. Among the better identified oceanographic barriers within the
642 Mediterranean are: the Gibraltar Strait and the Almeria-Oran Front- between
643 the Atlantic and Mediterranean basins, the Ibiza Channel and Balearic
644 Front- dividing the north- and southwestern Mediterranean sub-basins, the
645 Siculo-Tunisian Front between the western and eastern Mediterranean, and
646 the Otranto Strait and Aegean Front delimiting the Adriatic and Aegean
647 seas, respectively (e.g., Penant *et al*., 2013; Villamor *et al*., 2014; Riesgo *et*
648 *al*., 2016; Garcia-Cisneros *et al.*, 2016; and reviews in Paterno *et al.*, 2017
649 and Pascual *et al.*, 2017).

650 Nevertheless, these oceanographic fronts do not have equal effect on all
651 marine species. Pascual *et al.* (2017), reviewing published information for
652 70 species, found that the reduction of gene flow linked to the presence of

653 the abovementioned oceanographic fronts is more important in species with
654 long planktonic durations. This unexpected pattern is likely because these
655 larvae move off-shore, along the continental shelf and slope, and are thus
656 more affected by major oceanographic circulation and marine fronts than
657 larvae that remain close to the coastline (Pascual *et al.*, 2017). In our case,
658 we detected genetic divergence between both sides of the Almeria-Oran
659 front, as observed in other echinoderms (Calderón *et al*., 2012; Garcia-
660 Cisneros *et al*., 2016, 2017), although the divergence detected in Alboran
661 populations of *A. lixula* may actually be a transient process, as discussed
662 below for the temporal analyses, rather than a permanent one. Nevertheless,
663 we could not find any evidence of genetic divergence between the western
664 and eastern Mediterranean sub-basins, nor was there any significant
665 isolation by distance effect in the Mediterranean, a pattern that contrasts
666 with other echinoderms with large dispersal potential across the same
667 geographical area (e.g. Garcia-Cisneros *et al*., 2016, 2017). This may
668 suggest that *A. lixula* is not largely affected by discontinuities between the
669 Mediterranean populations, representing a well-mixed genetic pool within
670 this sea, and/or it reflects the recent evolutionary history within this basin,
671 marked by a demographic expansion (Wangensteen *et al*., 2012), with no
672 enough time to diverge within the Mediterranean basins.

673 The temporal genetic patterns among the two populations from at the
674 Atlantic-Mediterranean transition and the one from the north-western

675 Mediterranean indicate that populations were more divergent, particularly
676 Torremuelle (Alboran Sea), in 2009 than in 2014. Interannual variations in
677 the hydrological features along the Iberian Mediterranean shores are well
678 known (Pascual *et al.*, 2002; Pinot *et al.*, 2002; Bouffard *et al.*, 2010; Balbin
679 *et al.*, 2014), and have been held responsible for temporal patterns of genetic
680 variation in organisms such as the fish *Sardina pilchardus* (Olivar *et al.*,
681 2003), the sea urchin *Paracentrotus lividus* (Calderón *et al.*, 2012), or the
682 crab *Liocarcinus depurator* (Pascual *et al.*, 2016). In particular, in the
683 Alboran area, there is a complex structure with two main anticyclonic gyres
684 and a central cyclonic gyre (Sanchez-Vidal *et al.*, 2004; Sanchez-Garrido *et*
685 *al.*, 2013). The relative intensity of these gyres changes over time, and it
686 determines a temporally variable system of hydrological fronts in the area
687 (Renault *et al.*, 2012; Oguz *et al.*, 2014). These features affect the interplay
688 between Atlantic and Mediterranean waters, leading to variable patterns of
689 distribution of water masses in the Alboran Sea. This can explain our
690 finding of significant temporal genetic differences in Torremuelle and La
691 Herradura located in the Alboran Sea, while the northern population of
692 Colera, outside of this transitional area, remained more stable. Such
693 temporal changes in genetic composition of southern Iberian populations
694 relative to more northern populations were also detected for *Paracentrotus*
695 *lividus* (Calderón *et al.*, 2012). Torremuelle, in particular, lies in western
696 Alboran Sea, in a relatively isolated spot just outside the frontal system

generated by the western anticyclonic gyre (Sanchez-Garrido *et al.*, 2013; Oguz *et al.*, 2014). Thus, arrival of larvae to this locality is subject to stochastic and oceanographic changes among years, which may explain its higher genetic distance compared to other Mediterranean populations.

The effective population sizes (Ne) detected examining temporal variation in genetic composition were small (from tens to a few hundred individuals), and similar to Ne estimates for *P. lividus* (Calderón *et al.*, 2009). In this study, we did not specifically measure *A. lixula* abundances but information obtained from other studies showed densities that vary across space and time from low density-populations (0.2-0.3 individuals/ m^2) to densely populated sites (over 1.0 individuals/ m^2) (Palacín *et al*., 1998; Hereu *et al*., 2012). It is common for invertebrates and fish to have effective population sizes 2-6 orders of magnitude smaller than census sizes (Turner *et al.*, 2002; Hauser and Carvalho, 2008; Plough, 2016), which is often explained by large variance of reproductive success, whereby only few adults are able to produce successful progeny (sweepstake reproduction, Hedgecock, 1994). Statistic methods to calculate effective population size based on genetic data at two time points are appropriate to estimate contemporary Ne that reflects the effective number of parental specimens from which the collected sample comes from (e.g. Casilagan *et al*., 2013). Thus, the stochastic events that can take place during the reproduction together with the long planktonic period and the settlement and recruitment phases of *A. lixula* can likely explain the

719 small effective population sizes detected. It is noteworthy that the
720 hydrologically more stable northern population of Colera had ca. 6 to 10
721 times larger effective population sizes than the two southern populations.

722 From the last few years, there is increasing evidence of the importance of *A.*
723 *lixula* in the formation and maintenance of bare habitats (Bulleri *et al.*,
724 1999; Gianguzza *et al.*, 2011; Bonaviri *et al.*, 2011). *Arbacia lixula* is a
725 thermophilous species likely to be enhanced by warming temperatures
726 (Francour *et al.*, 1994; Gianguzza et al., 2011; Wangensteen, 2013a) and a
727 generalist species with a catholic diet that qualifies it as omnivore
728 (Wangensteen *et al.*, 2011; Agnetta *et al.*, 2013) no affected by a
729 commercial fishing industry. Thus, although some populations of A. *lixula*
730 at the Levant basin are in decline due to the ecosystem collapsing (Rilov
731 2016), under the current scenario of the ongoing tropicalization of the
732 Mediterranean, *A. lixula* can be favoured, leading to important changes in
733 ecosystem structure and functioning.

734 This study shows a main genetic break in *A. lixula* between both sides of the
735 Atlantic, and smaller differentiation signals associated with the Atlanto-
736 Mediterranean transition. However, no genetic structure was found within
737 the Mediterranean populations, suggesting that either the species' dispersal
738 abilities suffice to break the hydrological barrier separating the two
739 Mediterranean sub-basins and/or the genetic homogeneity is the result of the

recent evolutionary history of the species, although both hypotheses are not mutually exclusive. A picture of genetic homogeneity across the Mediterranean implies that the species may safely overcome occasional adverse local conditions and quickly replenish populations from neighbouring and distant locations. Future research, including whole-genome scans and the inclusion of populations from other areas (such as the Adriatic sea, Levant basin and/or the Atlantic African shores) will likely show a more nuanced picture of the underlying genetic structure associated with adaptation (e.g. Carreras *et al*., 2017). Overall, however, the patterns found suggest that the spread potential of *A. lixula* in the Mediterranean is large and the ongoing expansion of this thermophilous species will not be restricted by the potential impact of postulated barriers to gene flow.

DATA ARCHIVING

Data sets are available from Mendeley Datasets https://data.mendeley.com/ (to be completed upon acceptance).

ACKNOWLEDGEMENTS

This research was financially supported by the Spanish Government projects CTM2013-48163 and CTM2017-88080 and by a 'Juan de la Cierva' contract from the Spanish Government to RPP. We are indebted to Carlos

761 Renato Rezende Ventura for supplying us with the Brazilian samples, and to
762 Jacob González-Solís for providing the samples from Cape Verde.
763

764 **CONFLICT OF INTEREST**

765 The authors declare no conflict of interest.

766

767 Supplementary information is available at Heredity's website.

768

769 **REFERENCES**

770 Avise JC (2000). *Phylogeography: the history and formation of species*.
771 Harvard university press.
772 Addison JA, Hart MW (2005). Spawning, copulation and inbreeding
773 coefficients in marine invertebrates. *Biol Lett* **1**: 450–3.
774 Aglieri G, Papetti C, Zane L, Milisenda G, Boero F, Piraino S (2014). First
775 evidence of inbreeding, relatedness and chaotic genetic patchiness in
776 the holoplanktonic jellyfish *Pelagia noctiluca* (Scyphozoa, Cnidaria).
777 *PLoS One* **9**: e99647.
778 Agnetta D, Bonaviri C, Badalamenti F, Scianna C, Vizzini S, Gianguzza P
779 (2013). Functional traits of two co-occurring sea urchins across a
780 barren/forest patch system. *J Sea Res* **76**: 170–177.
781 Balbín R, López-Jurado JL, Flexas MM, Reglero P, Vélez-Velchí P,
782 González-Pola C, *et al.* (2014). Interannual variability of the early

783 summer circulation around the Balearic Islands: Driving factors and
784 potential effects on the marine ecosystem. *J Mar Syst* **138**: 70–81.

785 Beerli P, Felsenstein J (2001) Maximum likelihood estimation of a
786 migration matrix and effective population sizes in n subpopulations by
787 using a coalescent approach. *PNAS* **98**: 4563–4568.

788 Beerli P (2006) Comparison of Bayesian and maximum likelihood inference
789 of population genetic parameters. *Bioinformatics* **22**: 341–345.

790 Bonaviri C, Vega Fernández T, Fanelli G, Badalamenti F, Gianguzza P
791 (2011). Leading role of the sea urchin *Arbacia lixula* in maintaining the
792 barren state in southwestern Mediterranean. *Mar Biol* **158**: 2505–2513.

793 Borrero-Pérez GH, González-Wangüemert M, Marcos C, Pérez-Ruzafa A
794 (2011). Phylogeography of the Atlanto-Mediterranean sea cucumber
795 *Holothuria* (Holothuria) *mammata*: the combined effects of historical
796 processes and current oceanographical pattern. *Mol Ecol* **20**: 1964-
797 1975.

798 Boudouresque CF, Verlaque M, Azzolina JF, Meinesz A, Nédélec H, Rico
799 V (1989). Evolution des populations de *Paracentrotus lividus* et
800 d'*Arbacia lixula* (Echinoidea) le long d'un transect permanent à
801 Galeria (Corse). *rav Sci Parc Nat Rég Rés Nat Corse* **22**: 65–82.

802 Bouffard J, Pascual A, Ruiz S, Faugère Y, Tintoré J (2010). Coastal and
803 mesoscale dynamics characterization using altimetry and gliders: A
804 case study in the Balearic Sea. *J Geophys Res* **115**: C10029.

805 Broquet T, Viard F, Yearsley JM (2013). Genetic drift and collective
806 dispersal can result in chaotic genetic patchiness. *Evolution* **67**: 1660-
807 1675.

808 Bulleri F, Benedetti-Cecchi L, Cinelli F (1999). Grazing by the sea urchins
809 *Arbacia lixula* L. and *Paracentrotus lividus* Lam. in the Northwest
810 Mediterranean. *J Exp Mar Bio Ecol* **241**: 81–95.

811 Calderón I, Giribet G, Turon X (2008). Two markers and one history:
812 phylogeography of the edible common sea urchin *Paracentrotus*
813 *lividus* in the Lusitanian region. *Mar Biol* **154**: 137–151.

814 Calderón I, Palacín C, Turon X (2009). Microsatellite markers reveal
815 shallow genetic differentiation between cohorts of the common sea
816 urchin *Paracentrotus lividus* (Lamarck) in northwest Mediterranean.
817 *Mol Ecol* **18**: 3036–3049.

818 Calderón I, Pita L, Brusciotti S, Palacín C, Turon X (2012). Time and space:
819 genetic structure of the cohorts of the common sea urchin
820 *Paracentrotus lividus* in Western Mediterranean. *Mar Biol* **159**: 187–
821 197.

822 Carmona L, Malaquias MAE, Gosliner TM, Pola M, Cervera JL (2011).
823 Amphi-Atlantic distributions and cryptic species in Sacoglossan sea
824 slugs. *J Molluscan Stud* **77**: 401–412.

825 Carreras C, Ordóñez V, Zane L, Kruschel C, Nasto I, Macpherson E,
826 Pascual M (2017). Population genomics of an endemic Mediterranean
827 fish: differentiation by fine scale dispersal and adaptation. *Sci Rep* **7**:
828 43417.

829 Casilagan ILN, Juinio-Meñez MA, Crandall ED (2013). Genetic diversity,
830 population structure, and demographic history of exploited sea urchin
831 populations (*Tripneustes gratilla*) in the Philippines. *J Exp Mar Bio*
832 *Ecol* **449**: 284-293.

833 Chapuis M-P, Estoup A (2007). Microsatellite null alleles and estimation of
834 population differentiation. *Mol Biol Evol* **24**: 621–631.

835 Coll M, Piroddi C, Steenbeek J, Kaschner K, Ben Rais Lasram F, Aguzzi J,
836 *et al.* (2010). The biodiversity of the Mediterranean Sea: estimates,
837 patterns, and threats. *PLoS One* **5**: e11842.

838 Consuegra S, John E, Verspoor E, De Leaniz CG (2015). Patterns of natural
839 selection acting on the mitochondrial genome of a locally adapted fish
840 species. *Genet Sel Evol* **47**: 58.

841 Couvray S, Coupé S (2018). Three-year monitoring of genetic diversity
842 reveals a micro-connectivity pattern and local recruitment in the
843 broadcast marine species *Paracentrotus lividus*. *Heredity* **120**: 110

844 Deli T, Mohamed AB, Attia MHB, Zitari-Chatti R, Said K, Chatti N (2017).
845 High genetic connectivity among morphologically differentiated
846 populations of the black sea urchin *Arbacia lixula* (Echinoidea:
847 Arbacioida) across the central African Mediterranean coast. *Mar*
848 *Biodivers*: 10.1007/s12526-017-0832-y.

849 Do, C., Waples, R. S., Peel, D., Macbeth, G. M., Tillett, B. J. & Ovenden, J.
850 R. (2014). NeEstimator V2: re-implementation of software for the
851 estimation of contemporary effective population size (Ne) from genetic
852 data. *Mol Ecol Resour* **14**, 209-214.

853 Evanno G, Regnaut S, Goudet J (2005). Detecting the number of clusters of
854 individuals using the software structure: a simulation study. *Mol Ecol*
855 **14**: 2611–2620.

856 Excoffier L, Laval G, Schneider S (2005). Arlequin (version 3.0): an
857 integrated software package for population genetics data analysis. *Evol*
858 *Bioinform Online* **1**: 47–50.

859 Francour P, Boudouresque CF, Harmelin JG, Harmelin-Vivien ML,
860 Quignard JP (1994). Are the Mediterranean waters becoming warmer?
861 Information from biological indicators. *Mar Pollut Bull* **28**: 523–526.

862 Garcia-Cisneros A, Valero-Jiménez C, Palacín C, Pérez-Portela R (2013).
863 Characterization of thirty two microsatellite loci for three Atlanto-
864 Mediterranean echinoderm species. *Conserv Genet Resour* **5**: 749-753.

865 Garcia-Cisneros A, Palacín C, Khadra YB, Pérez-Portela R (2016). Low
866 genetic diversity and recent demographic expansion in the red starfish
867 *Echinaster sepositus* (Retzius 1816). *Sci Rep* **6**: 33269.

868 Garcia-Cisneros A, Palacín C, Ventura CRR, Feital B, Paiva PC, Pérez-
869 Portela R (2017). Intraspecific genetic structure, divergence and high
870 rates of clonality in an amphi-Atlantic starfish. *Mol Ecol* DOI:
871 10.1111/mec.14454.

872 Gerlach G, Jueterbock A, Kraemer P, Deppermann J, Harmand P (2010).
873 Calculations of population differentiation based on G(ST) and D:
874 forget G(ST) but not all of statistics! *Mol Ecol* **19**: 3845-3852.

875 Gianguzza P, Agnetta D, Bonaviri C, Di Trapani F, Visconti G, Gianguzza
876 F, *et al.* (2011). The rise of thermophilic sea urchins and the expansion
877 of barren grounds in the Mediterranean Sea. *Chem Ecol* **27**: 129–134.

878 Gianguzza P, Visconti G, Gianguzza F, Vizzini S, Sarà G, Dupont S (2014).
879 Temperature modulates the response of the thermophilous sea urchin
880 Arbacia lixula early life stages to CO2-driven acidification. *Mar*
881 *Environ Res* **93**: 70–77.

882 Glynn F, Houghton JD, Provan J (2015). Population genetic analyses reveal
883 distinct geographical blooms of the jellyfish *Rhizostoma octopus*
884 (Scyphozoa). *Biol J Linn Soc* **116***:* 582-592.

885 Hauser L, Carvalho GR (2008). Paradigm shifts in marine fisheries genetics:
886 ugly hypotheses slain by beautiful facts. *Fish Fish* **9**: 333–362.

887 Hedgecock D (1994). Does variance in reproductive success limit effective
888 population size of marine organisms? In: Beaumont A (ed) *Genetics*
889 *and evolution of aquatic organisms*, Chapman and Hall: London, pp
890 122–134.

891 Hereu B, Linares C, Sala E, Garrabou J, Garcia-Rubies A, Diaz D, Zabala
892 M (2012). Multiple processes regulate long-term population dynamics
893 of sea urchins on Mediterranean rocky reefs. *PloS one* **7**: e36901.

894 Jombart T (2008). adegenet: a R package for the multivariate analysis of
895 genetic markers. *Bioinformatics* **24**: 1403–1405.

896 Jombart T, Devillard S, Balloux F (2010). Discriminant analysis of principal
897 components: a new method for the analysis of genetically structured
898 populations. *BMC Genet* **11**: 94.

899 Jones CG, Lawton JH, Shachak M (1994). Organisms as ecosystem
900 engineers. In: *Ecosystem Management*, Springer New York: New
901 York, NY, pp 130–147.

902 Jones CG, Lawton JH, Shachak M (1997). Positive and negative effects of
903 organisms as physical ecosystem engineers. *Ecology* 78: 1946-1957

904 Jorde E, Ryman N (1995) Temporal allele frequency change and estimation
905 of effective size in populations with overlapping generations. *Genetics*
906 139: 1077-1090.
907 Jorde PE, Ryman N (2007). Unbiased estimator for genetic drift and
908 effective population size. *Genetics* **177**: 927–935.
909 Jost L (2008). G_{ST} and its relatives do not measure differentiation. *Mol Ecol*
910 **17**: 4015–4026.
911 Kempf M (1962). Recherches d'écologie comparée sur *Paracentrotus*
912 *lividus* (Lmk.) et *Arbacia lixula* (L.). *Rec Trav Stat Mar Endoume* **25**:
913 47–116.
914 Kopelman NM, Mayzel J, Jakobsson M, Rosenberg NA, Mayrose I (2015).
915 Clumpak : a program for identifying clustering modes and packaging
916 population structure inferences across *K*. *Mol Ecol Resour* **15**: 1179–
917 1191.
918 Kroh A, Smith AB (2010). The phylogeny and classification of post-
919 Palaeozoic echinoids. *J Syst Palaeontol* **8**: 147–212.
920 Lejeusne C, Chevaldonné P, Pergent-Martini C, Boudouresque CF, Pérez T
921 (2010). Climate change effects on a miniature ocean: the highly
922 diverse, highly impacted Mediterranean Sea. *Trends Ecol Evol* **25**:
923 250–260.

924 Lessios HA, Kessing BD, Pearse JS (2001). Population structure and
925 speciation in tropical seas: global phylogeography of the sea urchin
926 *Diadema*. *Evolution* **55**: 955-975.
927 Lessios HA, Lockhart S, Collin R, Sotil G, Sánchez-Jerez P, Zigler KS, *et*
928 *al.* (2012). Phylogeography and bindin evolution in *Arbacia*, a sea
929 urchin genus with an unusual distribution. *Mol Ecol* **21**: 130–144.
930 Ling SD, Scheibling RE, Rassweiler A, Johnson CR, Shears N, Connell SD,
931 *et al.* (2014). Global regime shift dynamics of catastrophic sea urchin
932 overgrazing. *Phil Trans R Soc B Biol Sci* **370**: 20130269–20130269.
933 Madeira P, Kroh A, Cordeiro R, Meireles R, Avila SP (2011). The fossil
934 echinoids of Santa Maria Island, Azores (Northern Atlantic Ocean).
935 *Acta Geol Pol* **61**: 243-264
936 Metz EC, Gomez-Gutierrez G, Vacquier VD (1998). Mitochondrial DNA
937 and bindin gene sequence evolution among allopatric species of the sea
938 urchin genus *Arbacia*. *Mol Biol Evol* **15**: 185–195.
939 Mortensen T (1935). *A Monograph of the echinoidea II: Bothriocidaroida,*
940 *Melonechinoida, Lepidocentroida and Stirodonta*. C.A. Reitzel:
941 Copenhagen.
942 Narum SR (2006). Beyond Bonferroni: Less conservative analyses for
943 conservation genetics. *Conserv Genet* **7**: 783–787.

944 Nei M, Tajima F (1981). Genetic drift and estimation of effective population
945 size. *Genetics* **98**: 625–40.

946 Oguz T, Macias D, Garcia-Lafuente J, Pascual A, Tintore J (2014). Fueling
947 plankton production by a meandering frontal jet: a case study for the
948 Alboran Sea (Western Mediterranean). *PLoS One* **9**: e111482.

949 Olivar MP, Catalán IA, Emelianov M, Fernández de Puelles ML (2003).
950 Early stages of *Sardina pilchardus* and environmental anomalies in the
951 Northwestern Mediterranean. *Est Coast Shelf Sci* **56**: 609-19.

952 Palacín C, Turon X, Ballesteros M, Giribet G, López S (1998a). Stock
953 Evaluation of three littoral echinoid species on the Catalan Coast
954 North-Western Mediterranean. *Mar Ecol* **19:** 163-177.

955 Pascual A, Buongiorno Nardelli B, Larnicol G, Emelianov M, Gomis D
956 (2002). A case of an intense anticyclonic eddy in the Balearic Sea
957 (western Mediterranean). *J Geophys Res* **107**: 3183.

958 Pascual M, Palero F, García-Merchán VH, Macpherson E, Robainas-Barcia
959 A, Mestres F, *et al.* (2016). Temporal and spatial genetic differentiation
960 in the crab *Liocarcinus depurator* across the Atlantic-Mediterranean
961 transition. *Sci Rep* **6**: 29892.

962 Pascual M, Rives B, Scgunter C, Macpherson E (2017). Impact of life
963 history traits on gene flow: A multispecies systematic review across

964 oceanographic barriers in the Mediterranean Sea. *PLoS One* **12**:
965 e0176419.

966 Peakall R, Smouse PE (2006). GENALEX 6: Genetic analysis in Excel.
967 Population genetic software for teaching and research. *Mol Ecol Notes*
968 **6**: 288–295.

969 Pérez-Portela R, Villamor A, Almada V (2010). Phylogeography of the sea
970 star *Marthasterias glacialis* (Asteroidea, Echinodermata): deep
971 genetic divergence between mitochondrial lineages in the north-
972 western Mediterranean. *Mar Biol* **157**: 2015-2028.

973 Pérez-Portela R, Turon X, Bishop J DD (2012). Bottlenecks and loss of
974 genetic diversity: spatio-temporal patterns of genetic structure in an
975 ascidian recently introduced in Europe. *Mar Ecol Prog Ser* **451**: 93-
976 105.

977 Pérez-Portela R, Rius M, Villamor A (2017). Lineage splitting, secondary
978 contacts and genetic admixture of a widely distributed marine
979 invertebrate. *J Biogeogr* **44**: 446–460.

980 Petit G, Delamare-Deboutteville, C. Bougis P (1950). Le fichier faunistique
981 du laboratoire Arago. *Vie Milieu Série A Biol Mar* **1**: 356-360.

982 Pineda MC, Turon X, Pérez-Portela R, López-Legentil S (2016). Stable
983 populations in unstable habitats: temporal genetic structure of the
984 introduced ascidian *Styela plicata* in North Carolina. *Mar Biol* **163**: 59.

985 Pinot JM, López-Jurado J., Riera M (2002). The CANALES experiment
986 (1996-1998). Interannual, seasonal, and mesoscale variability of the
987 circulation in the Balearic Channels. *Prog Oceanogr* **55**: 335–370.

988 Plough L V. (2016). Genetic load in marine animals: a review. *Curr Zool*
989 **62**: 567–579.

990 Pollak E (1983). A new method for estimating the effective population size
991 from allele frequency changes. *Genetics* **104**: 531–48.

992 Pritchard JK, Stephens M., Donnelly P (2000). Inference of population
993 structure using multilocus genotype data. *Genetics* **155**: 945–959.

994 Privitera D, Noli M, Falugi C, Chiantore M (2011). Benthic assemblages
995 and temperature effects on *Paracentrotus lividus* and *Arbacia lixula*
996 larvae and settlement. *J Exp Mar Bio Ecol* **407**: 6–11.

997 Raymond M, Rousset F (1995). GENEPOP: a population genetics software
998 for exact tests and ecumenism. Vers. 1.2. *J Hered* **86**: 248–249.

999 Renault L, Oguz T, Pascual A, Vizoso G, Tintore J (2012). Surface
1000 circulation in the Alborán Sea (western Mediterranean) inferred from
1001 remotely sensed data. *J Geophys Res Ocean* **117**: n/a-n/a.

1002 Riesgo A, Pérez-Portela R, Pita L, Blasco G, Erwin P M, López-Legentil S
1003 (2016). Population structure and connectivity in the Mediterranean
1004 sponge *Ircinia fasciculata* are affected by mass mortalities and
1005 hybridization. *Heredity* **117**: 427.

1006 Rilov G (2016). Multi-species collapses at the warm edge of the warming
1007 sea. *Sci Rep* **6**: 36897.

1008 Sánchez-Garrido JC, García Lafuente J, Álvarez Fanjul E, Sotillo MG, de
1009 los Santos FJ (2013). What does cause the collapse of the Western
1010 Alboran Gyre? Results of an operational ocean model. *Prog Oceanogr*
1011 **116**: 142–153.

1012 Sanchez-Vidal A, Calafat A, Canals M, Fabres J (2004). Particle fluxes in
1013 the Almeria-Oran Front: control by coastal upwelling and sea surface
1014 circulation. *J Mar Syst* **52**: 89–106.

1015 Silva G, Lima FP, Martel P, Castilho R (2014). Thermal adaptation and
1016 clinal mitochondrial DNA variation of European anchovy. *P Roy Soc*
1017 *Lond B Biol* **281:** 20141093.

1018 Stefanini G (1911). Di alcune *Arbacia* fossili. *Riv Ital di Paleontol* **17**: 51–
1019 52.

1020 Taboada S, Pérez-Portela R (2016). Contrasted phylogeographic patterns on
1021 mitochondrial DNA of shallow and deep brittle stars across the
1022 Atlantic-Mediterranean area. *Sci Rep* **6**: 32425.

1023 Team R Core (2013). A language and environment for statistical computing.

1024 Tommasi LR (1964). Observações sôbre Equinóides do Brasil. *Rev Bras*
1025 *Biol* **24**: 83–93.

1026 Tortonese E (1965). *Fauna d'Italia: Vol. VI, Echinodermata* (Calderini,
1027 Ed.). Bologna.

1028 Turner TF, Wares JP, Gold JR (2002). Genetic effective size is three orders
1029 of magnitude smaller than adult census size in an abundant, Estuarine-
1030 dependent marine fish (*Sciaenops ocellatus*). *Genetics* **162**: 1329–39.

1031 Villamor A, Costantini F, Abbiati M (2014). Genetic structuring across
1032 marine biogeographic boundaries in rocky shore invertebrates. *PLoS*
1033 *One* **9**: e101135.

1034 Visconti G, Gianguzza F, Butera E, Costa V, Vizzini S, Byrne M, *et al.*
1035 (2017). Morphological response of the larvae of *Arbacia lixula* to near-
1036 future ocean warming and acidification. *ICES J Mar Sci* **74**: 1180–
1037 1190.

1038 Wangensteen OS, Turon X, García-Cisneros A, Recasens M, Romero J,
1039 Palacín C (2011). A wolf in sheep's clothing: carnivory in dominant
1040 sea urchins in the Mediterranean. *Mar Ecol Prog Ser* **441**: 117-128

1041 Wangensteen OS, Turon X, Pérez-Portela R, Palacín C (2012). Natural or
1042 Naturalized? Phylogeography suggests that the abundant sea urchin
1043 *Arbacia lixula i*s a recent colonizer of the Mediterranean. *PLoS One* **7**:
1044 e45067.

1045 Wangensteen OS (2013). Biology and phylogeography of the black sea
1046 urchin *Arbacia lixula* (Echinoidea: Arbacioida). PhD thesis. University
1047 of Barcelona.

1048 Wangensteen OS, Dupont S, Casties I, Turon X, Palacín C (2013a). Some
1049 like it hot: Temperature and pH modulate larval development and
1050 settlement of the sea urchin *Arbacia lixula*. *J Exp Mar Bio Ecol* **449**:
1051 304-311

1052 Wangensteen OS, Turon X, Casso M, Palacín C (2013b). The reproductive
1053 cycle of the sea urchin *Arbacia lixula* in northwest Mediterranean:
1054 potential influence of temperature and photoperiod. *Mar Biol* **160**:
1055 3157–3168.

1056 Yeruham E, Rilov G, Shpigel M, Abelson A (2015). Collapse of the
1057 echinoid Paracentrotus lividus populations in the Eastern Mediterranean
1058 result of climate change?. *Sci Rep* **5**: 13479.

1059 Zigler KS, Lessios HA (2003). 250 million years of bindin evolution. *Biol*
1060 *Bull* **205**: 8–15.

1061 Zigler KS, McCartney MA, Levitan DR, Lessios HA (2005). Sea urchin
1062 bindin divergence predicts gamete compatibility. *Evolution* **59**: 2399.

1063

1064 **TITLES AND LEGENDS TO FIGURES**

1065

Figure 1. Collection sites and general genetic structure in *Arbacia lixula*. A) Sampling sites and pie charts of the percentage of each cluster (K=3) per site obtained from STRUCTURE as represented below, and B) STRUCTURE barplot with the posterior probabilities of individual assignment of the most probable number of clusters for the whole dataset (K=3). Clusters are represented by different colours (yellow, red and blue), and each bar represents a different individual. Numbers and red lines represent the four different marine barriers considered: Mid-Atlantic barrier (1), Gibraltar Strait (2), Almeria Oran front (3) and Siculo-Tunisian Strait (4).

Figure 2. Genetic differentiation between sites in *Arbacia lixula*. A) Heatmap and dendrogram based on pairwise F_{ST} values, and B) heatmap and dendrogram based on pairwise D_{est} values. Values of F_{ST} and D_{est} and their associated p-values are included as Supplementary Table S2.
* Highlights the different clustering of Torremuelle (Tor) with other marine areas between heatmaps.

Figure 3. DAPCs of *Arbacia lixula*. Graphs represent DAPC results from three different analyses: A) the whole dataset, B) eastern Atlantic and Mediterranean sites, and C) only Mediterranean sites (including the Alboran Sea). On the graph, points represent different individuals, and point patterns

different sampling sites. Blue pattern= Mediterranean sites; red-orange pattern= eastern Atlantic; and yellow pattern= western Atlantic.

Figure 4. Genetic differences over time in *Arbacia lixula*. A) Heatmaps based on F_{ST} (left) and D_{est} (right) values between years and three sites, and B) DAPC analyses for the three populations at two time points (2009 and 2014).

SUPPLEMENTARY FIGURES

Supplementary S1. Allele diversity in *Arbacia lixula*. Allele richness and percentage of private alleles (Np %) from three major marine areas: Mediterranean Sea, Eastern Atlantic and Western Atlantic areas.

Supplementary S2. Potential effect of missing data on $F_{IS.}$ Graph representing the relationship between the fixation index F_{IS} and number of missing alleles in *Arbacia lixula*.

Supplementary S3. Optimal number of clusters (K=3) from STRUCTURE according to the *ad hoc* statistic K (Delta K).

Supplementary S4. Genetic clustering from "adegenet" in *Arbacia lixula*. A) BIC values versus number of clusters from 1 to 13; the optimal number of clusters according to BIC values is 6, and B) barplot from the *Compoplot* analysis according to 6 clusters; coloured bars represent the membership probability to each cluster for every individual.

Supplementary S5. Mantel test results in *Arbacia lixula*. Correlation between genetic distance ($F_{ST}/1-F_{ST}$) and geographical distance (km) for: A) the whole dataset, B) eastern Atlantic and Mediterranean Sea, and C) only the Mediterranean Sea.

Code	Locality	Geographical area	N	Ho	He	F_{IS}	Allele
Cre	Crete	Eastern Mediterranean	24	0.565± 0.195	0.849± 0.076	0.323± 0.07 *	13.2± 1.23
Kos	Kos	Eastern Mediterranean	24	0.597± 0.236	0.854 ± 0.059	0.289± 0.08*	12.6±1 .26
Sic	Sicilia	Eastern Mediterranean	24	0.568± 0.213	0.879 ± 0.051	0.343± 0.08 *	12.8± 1.39
Pop	Populonia	Western Mediterranean	24	0.522± 0.222	0.842 ± 0.059	0.365± 0.09 *	11.2± 0.96
Col	Colera (2009)	Western Mediterranean	24	0.562± 0.198	0.878 ± 0.029	0.347± 0.07 *	13.4± 1.02
Ben	Benidorm	Western Mediterranean	24	0.563± 0.215	0.864 ± 0.058	0.331± 0.08 *	12.1± 1.07
Her	La Herradura (2009)	Alboran Sea	24	0.552± 0.134	0.819 ± 0.103	0.300± 0.06 *	11.9± 1.06
Tor	Torremuelle (2009)	Alboran Sea	24	0.571± 0.205	0.845 ± 0.065	0.300± 0.09 *	11.8± 1.20
		MEDITERRANEAN	192	0.563±0.090	0.863± 0.052	-	(10.94± 0.80)
Fai	Faials, Azores	Macaronesian Island, eastern Atlantic	24	0.619± 0.202	0.834 ± 0.064	0.241± 0.08 *	11.7± 1.01
Gig	Los Gigantes, Tenerife	Macaronesian Island, eastern Atlantic	24	0.569± 0.232	0.852 ± 0.051	0.289± 0.08 *	13.1± 1.26
Cav	Boavista, Cape Verde	Macaronesian Island, eastern Atlantic	24	0.585± 0.222	0.872 ± 0.057	0.318± 0.08 *	14.3± 1.28
		EASTERN ATLANTIC	72	0.591± 0.200	0.856± 0.051	-	(11.10± 0.71)
Cfr	Cabo Frío	Brazil, western Atlantic	16	0.625± 0.282	0.804 ± 0.122	0.201± 0.11 *	9.3± 1.06
Ita	Itaipu	Brazil, western Atlantic	22	0.579± 0.209	0.819 ± 0.113	0.253± 0.06 *	11.0± 1.12
		WESTERN ATLANTIC	38	0.593± 0.205	0.803± 0.100	-	(9.76± 0.91)
Col 2014	Colera (2014)	Western Mediterranean	25	0.625± 0.082	0.869 ± 0.015	0.267± 0.09 *	13.0± 0.91
Her 2014	La Herradura (2014)	Alboran Sea	27	0.588± 0.083	0.858 ± 0.017	0.298± 0.09 *	12.6± 1.18
Tor 2014	Torremuelle (2014)	Alboran Sea	25	0.627± 0.069	0.861 ± 0.014	0.255 ± 0.08 *	12.7± 1.02

Table 1. Genetic descriptors of *Arbacia lixula*. Codes of the populations including the year of collection for the populations used for the temporal analyses, localities, geographical area, sample size (N), heterozygosity observed (Ho), heterozygosity expected (He), inbreeding coefficient (F_{IS}), and allele diversity- mean number of alleles per population or allele richness per marine geographical area in brackets (calculated by rarefaction from the minimum sample size). Standard error is also presented for genetic descriptors. * Significant HW disequilibrium ($p< 0.01$).

SOURCE OF VARIATION	D.F.	FIXATION INDEX	% VARIATION	P-VALUE	GROUPING
Brazil, Macaronesia, Mediterranean					
Among group (3 groups, 13 populations)	2	F_{CT}: 0.033	3.30	0.000 **	1. Ita, Cfr
Among populations within groups	10	F_{SC}: 0.008	0.80	0.000 **	2. Fai, Gig, Cav
Within populations	298	F_{IS}: 0.306	29.32	0.000 **	3. Ben, Col, Pop, Sic, Cre, Kos, Tor, Her
Within individuals	302	F_{IT}: 0.334	66.58	0.000 **	
TOTAL	603				
Macaronesia - Mediterranean					
Among group (2 groups, 11 populations)	1	F_{CT}: 0.013	1.30	0.006 **	1. Fai, Gig, Cav
Among populations within groups	9	F_{SC}: 0.009	0.87	0.000 **	2. Ben, Col, Pop, Sic, Cre, Kos, Tor, Her
Within populations	253	F_{IS}: 0.309	30.32	0.000 **	
Within individuals	264	F_{IT}: 0.325	67.51	0.000 **	
TOTAL	527				
Mediterranean - Alboran sea					
Among group (2 groups, 8 populations)	1	F_{CT}: 0.005	0.54	0.088	1. Ben, Col, Pop, Sic, Cre, Kos
Among populations within groups	6	F_{SC}: 0.006	0.60	0.002 **	2. Tor, Her
Within populations	184	F_{IS}: 0.320	31.61	0.000 **	
Within individuals	192	F_{IT}: 0.327	67.26	0.000 **	
TOTAL	383				
western Mediterranean - eastern Mediterranean					
Among group (2 groups, 6 populations)	1	F_{CT}: 0.001	0.13	0.393	1. Ben, Col, Pop
Among populations within groups	4	F_{SC}: 0.001	0.03	0.472	2. Sic, Cre, Kos
Within populations	138	F_{IS}: 0.326	32.58	0.000 **	
Within individuals	144	F_{IT}: 0.327	67.26	0.000 **	
TOTAL	287				

Table 2. Analyses of the Molecular Variance (AMOVA) in *A. lixula*. Four different groupings and subsets of populations are represented. Populations comprising each group are listed on the right column. * Significant at $p<0.05$; ** Significant at $p< 0.01$.

Migration direction	Mean	Confidence interval
Mediterranean→E Atlantic	**24.182**	**(5.333- 42.667)**
E Atlantic → Mediterranean	13.042	(0.000- 29.333)
Mediterranean → W Atlantic	**18.336**	**(0.667- 35.333)**
W Atlantic → Mediterranean	7.145	(0.000- 24.000)
E Atlantic → W Atlantic	8.629	(0.000- 24.667)
W Atlantic → E Atlantic	14.919	(0.000- 33.333)

Table 3. Migration patterns in *A. lixula*. Mutation-scaled effective migration rates (M) between three marine areas: western Atlantic (W Atlantic), Eastern Atlantic (E Atlantic) and Mediterranean Sea. Mean values of M and the 95% interval of confidence are presented in the table

Per pop / Temporal methods	Pollak	Nei/Tajima	Jorde/Ryman
Colera	177.3 (56.5 - ∞)	268.3 (67 - ∞)	387.9 (264.5 - 534.5)
La Herradura	33.9 (18.1 - 66.6)	38.2 (19.9 - 78.8)	35.3 (23.2 - 50)
Torremuelle	34.2 (19.3 - 63.3)	38.8 (21.4 - 75.5)	38.1 (26.3 - 52.2)

Table 4. Estimated values of effective population size using three different temporal method estimates. Values within parentheses represent the 95% confidence interval of the estimates.

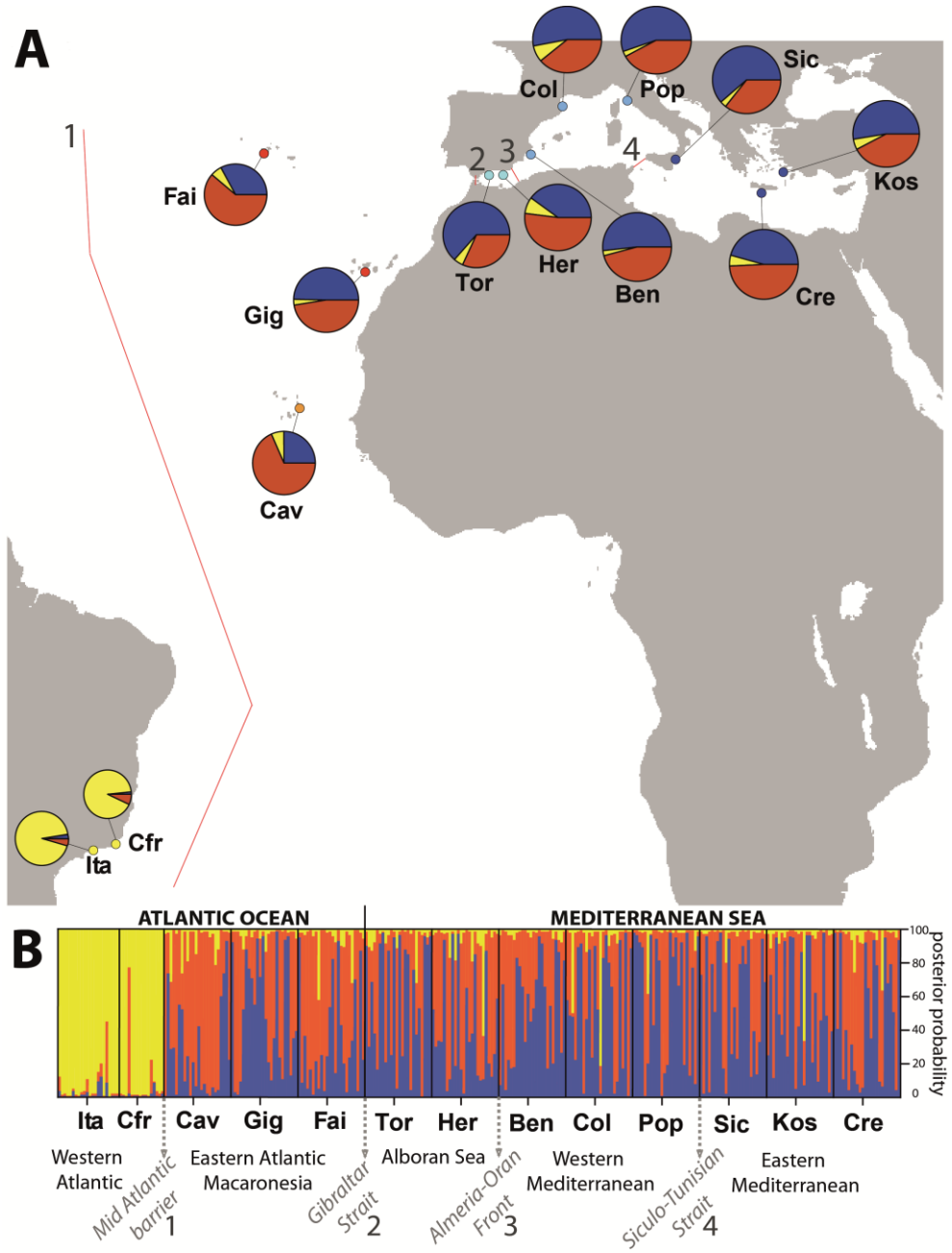

1157

1158 Figure 1

1159

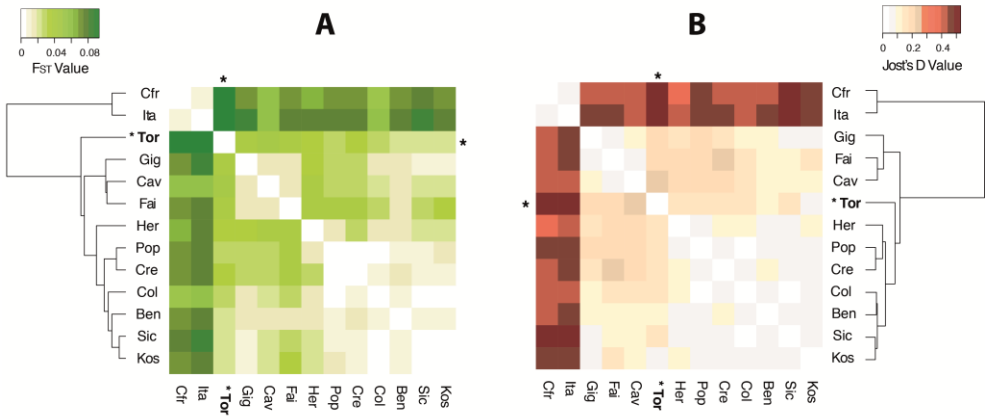

1160

1161

1162 Figure 2

1163

1164 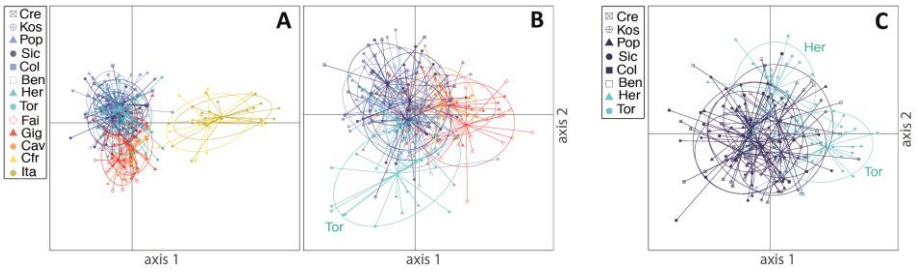

1165

1166 Figure 3

1167

1168

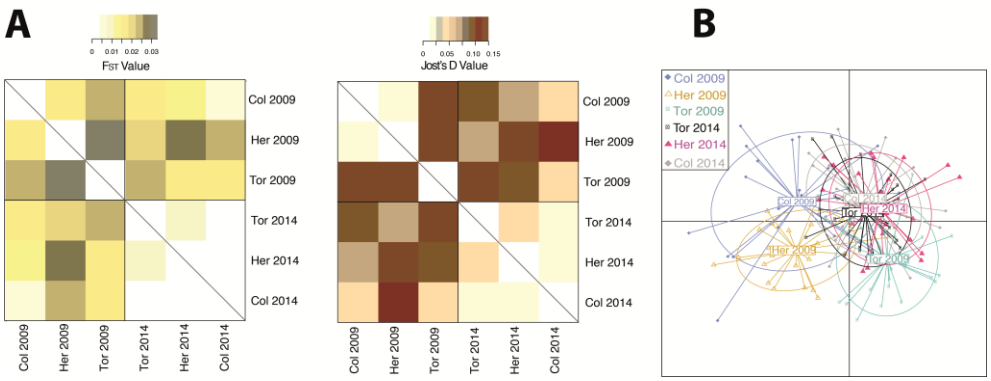

1169

1170

1171 Figure 4